Article

Tetrazenyl-, Imido-, and Azidoaluminate Derivatives of a Sterically Demanding Bis-Silazide Ligand

Han-Ying Liu, Ryan J. Schwamm, Jakub Kenar, Mary F. Mahon and Michael S. Hill *

Department of Chemistry, University of Bath, Claverton Down, Bath BA2 7AY, UK; hyl219@bath.ac.uk (H.-Y.L.); ryan.schwamm@gmail.com (R.J.S.); kubakenar.kk@gmail.com (J.K.); chsmfm@bath.ac.uk (M.F.M.)
* Correspondence: msh27@bath.ac.uk

Abstract: The potassium alumanyl $[\{SiN^{Dipp}\}AlK]_2$ ($SiN^{Dipp} = \{CH_2SiMe_2NDipp\}_2$; Dipp = $2,6\text{-}i\text{-}Pr_2C_6H_3$) reacts with organic azides via reductive N_2 elimination. With the less sterically encumbered azides PhN_3 and $C_{10}H_{15}N_3$ (1-azidoadamantane), the putative initially formed aluminium imide undergoes facile [2 + 3] cycloaddition to provide the tetrazenylaluminates $[\{SiN^{Dipp}\}Al\text{-}\kappa^2\text{-}N,N'\text{-}(\{N(R)\}_2N_2)]K$ (R = Ph, $C_{10}H_{15}$). In contrast, each Al(I) centre of $[\{SiN^{Dipp}\}AlK]_2$ only reacts with a single equivalent of $2,4,6\text{-}Me_3C_6H_2N_3$ to provide the imidoaluminate $[\{SiN^{Dipp}\}AlN(2,4,6\text{-}Me_3C_6H_2)(K\cdot C_6H_6)]$, which crystallises as a monomer and displays a short Al-N distance of 1.7040(13) Å. Attempts to synthesise the azide $[\{SiN^{Dipp}\}AlN_3]$ by reaction of $[\{SiN^{Dipp}\}AlI]$ with an excess of KN_3 resulted in exclusive formation of the bis(azido)aluminate $[\{SiN^{Dipp}\}Al(N_3)_2K]$, which crystallises as an infinite 1-dimensional polymer propagated by $\mu\text{-}(1,3)\text{-}N_3$ bridging interactions between the potassium cations and azide anions. Although the THF-adducted azide $[\{SiN^{Dipp}\}AlN_3(THF)]$ may be synthesised and characterised by more stringent control of the reaction stoichiometry, the synthetic viability of this route remains compromised by competitive generation of $[\{SiN^{Dipp}\}Al(N_3)_2K]$.

Keywords: Al(I); azide; imide; tetrazene

1. Introduction

Motivated by both their practical potential (e.g., as precursors to nitride materials) [1,2] or to address more fundamental questions of main group heteronuclear multiple bonding [3–6], the chemistry of nitrogen-bonded aluminium compounds has attracted longstanding attention [7,8]. Initial studies of oligomeric aluminium imides, $[RAlNR']_n$, demonstrated that systems comprising less sterically demanding organic substituents may be isolated as cage structures with alternating Al and N vertices and with a topology dictated by the identity of R and R' [9–12]. Despite the introduction of various more sterically demanding organic residues at either, or both, of the constituent aluminium or nitrogen centres that allowed the synthesis of several dimeric iminoalanes with Al_2N_2 cores [5,13–16], monomeric analogues long continued to prove elusive.

Roesky and co-workers demonstrated in 2001 that, while reactions of various triorganosilyl azides with the sterically encumbered Al(I) species [(BDI)Al:] (**I**: BDI = $HC[(Me)CNDipp]_2$; Dipp = $2,6\text{-}i\text{-}Pr_2C_6H_3$) provided the requisite elimination of dinitrogen, the resultant transient imides were insufficiently stabilised to prevent the [2 + 3] cycloaddition of a further azide equivalent to provide aluminatetrazene species (**II–IV**, Figure 1a) [17,18]. Although the aluminium species could not be structurally characterised in the solid state, by analogy to its heavier congener [(BDI)Ga=N(2,6-Trip₂C₆H₃)], Power

and co-workers' use of the very sterically encumbered azide 2,6-Trip$_2$C$_6$H$_3$N$_3$ (Trip = 2,4,6-*i*-Pr$_3$C$_6$H$_2$) confirmed that the kinetic stabilisation of the Al=N linkage could be achieved [19]. A further indication of the reactivity intrinsic to the terminal Al-N bond was provided by a subsequent report of the behaviour of **I** toward the less sterically demanding *m*-terphenyl azide 2,6-Dipp$_2$C$_6$H$_3$N$_3$ which underwent C-H activation of a flanking methyl group [19,20]. The first structurally characterised terminal aluminium imide (**V**, Figure 1b) resulted serendipitously from β-diketiminate ligand degradation after treatment of a *tert*-butyl-substituted analogue of **I** with the *N*-heterocyclic carbene 1,3-di-isopropyl-4,5-dimethyl-2-ylidene [21]. Although **V** was shown to comprise a short Al-N bond [1.705(2) Å], crystallographic verification of rationally accessed imide species has only been realised during the past half-decade. Effectively simultaneous reports from the groups of Coles and Aldridge described the anionic imide units of compounds **VI** and **VIIa** that were accessed by the respective treatment of the potassium alumanyls K$_2$[Al(NON)]$_2$ (**VIII** [22], NON = [O(SiMe$_2$NDipp)$_2$]$^{2-}$) [23–25] and K$_2$[Al(NON^{xanth})]$_2$ (**IX** [26], NON^{xanth} = 4,5-bis(2,6-diisopropylanilido)-2,7-di-tert-butyl-9,9-dimethyl-xanthene) [27–30], with 2,4,6-Me$_3$C$_6$H$_2$N$_3$ and DippN$_3$. This protocol was subsequently extended by Aldridge and co-workers to the synthesis of a variety of analogous, but more labile, silyl- and borylimido derivatives (**VIIb–VIId**) [30]. Compounds **VI** and **VIIa–VIId** presented similarly short terminal Al-N bond lengths (**VI**, 1.7251(11); **VIIa**, 1.723(2); **VIIb** 1.730(6); **VIIc** 1.7304(15); **VIId** 1.739(3) Å) that were initially formulated as multiple Al=N bonds. The calculated Wiberg bond indices (WBI, ca. 0.6), however, implicated minimal potential for π bonding such that the molecules are better represented with the ionic formulations depicted in Figure 1 [30]. The current lower limit to any Al-N bond length was subsequently achieved by Power's characterisation of the charge neutral species Ar′Al≡NAr″ [**X**, Ar′ = C$_6$H-2,6-(C$_6$H$_2$-2,4,6-*i*-Pr$_3$)$_2$-3,5-*i*-Pr$_2$; Ar″ = C$_6$H$_3$-2,6-(C$_6$H$_2$-2,4,6-Me$_3$)$_2$] [31]. In this case, the extreme kinetic protection afforded by both the Al-bound Ar′ and N-bound Ar″ substituents impose an unperturbed linear geometry to the C-Al=N-C unit and a resultant contraction of the Al-N bond distance to 1.625(4) Å. Although dispersion-corrected DFT calculations performed on **X** attributed a combination of one σ- and two π-type components to the Al-N bonding, even here the 90% electron localisation on the N atom yielded a consequent WBI of only 0.89.
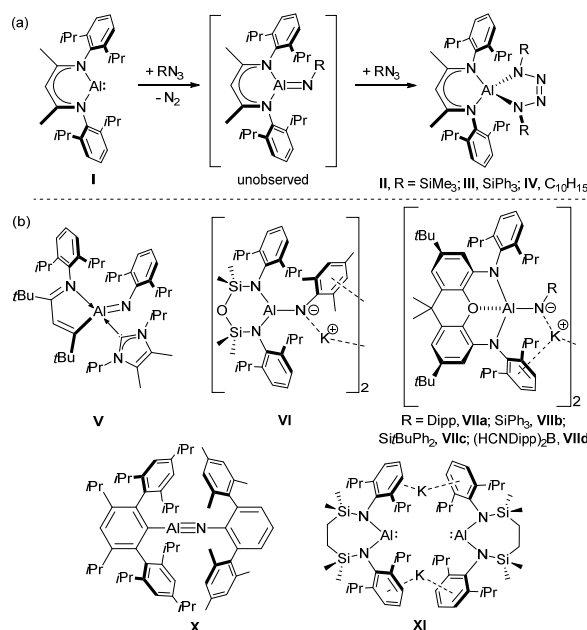

Figure 1. (**a**) Reactivity of **I** toward RN$_3$ and the synthesis of compounds **II–IV**; (**b**) the structures of compounds **V**, **VI**, **VIIa-d**, **X**, and **XI**.

Against this backdrop, our own recent observations have centred on the potassium alumanyl reagent (**XI**) [32], which is supported by the sterically demanding $\{SiN^{Dipp}\}^{2-}$ dianion (SiN^{Dipp} = $\{CH_2SiMe_2NDipp\}_2$) and acts as a potent but kinetically discriminating two-electron reductant toward multiply bonded organic and inorganic small molecule substrates [33–37]. In this contribution, we extend our study of **XI** to its reactivity with organic azides and describe our unsuccessful attempts to synthesise molecular Al-μ-N-Al-bridged derivatives of the nitride (N^{3-}) anion by reaction of **XI** with azidoaluminium species which are also supported by the $\{SiN^{Dipp}\}^{2-}$ dianion.

2. Results and Discussion

In common with many reactions of the azide functional group at low oxidation state *p*-block element centres [38], treatment of **XI** with the less sterically demanding azidobenzene and azidoadamantantane induced visible N_2 elimination. In a manner reminiscent of the reactivity of **I** (Figure 1a) [17,18] and **IX** with Me_3SiN_3 [27], and Power and co-workers' observations of the one-coordinate alanediyl precursor to compound **X** with azidoadamantantane [31], the presumed phenyl- and adamantylimidoaluminium intermediates undergo immediate [2 + 3] cycloaddition with a further equivalent of azide to provide the respective tetrazene derivatives, **1** and **2** (Scheme 1).
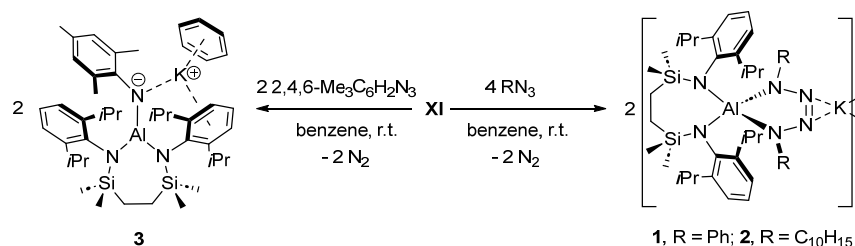
Scheme 1. Synthesis of compounds **1–3**.

Compound **1** was soluble in C_6D_6 and displayed a series of $\{SiN^{Dipp}\}$ ligand resonances in its ^1H and $^{13}C\{^1H\}$ NMR spectra consistent with the retention of a C_{2v}-symmetric chelate structure. In contrast, compound **2** rapidly deposited as a colourless amorphous solid from the benzene reaction solvent, necessitating the use of d_8-THF to record solution-state NMR data. Under these conditions, the resultant ^1H NMR spectrum evidenced a lowering of symmetry that results in a diastereotopic disposition of the $\{SiN^{Dipp}\}$ *iso*-propyl methyl substituents that is most clearly evidenced by a splitting of the corresponding methine environments, which resonated as a pair of equally intense (2H by relative integration) multiplets at δ 4.21 and 4.09 ppm. Single crystals suitable for X-ray diffraction analysis were, thus, obtained either from *n*-hexane (**1**) or by slow diffusion of the same alkane solvent into a THF solution (**2**). The results of these analyses are shown in Figures 2 and 3, respectively, while selected bond length and angle data for both compounds are presented in Table 1.

Table 1. Selected bond lengths (Å) and angles (°) for compounds **1–5**.

	1	2	3	4	5
Al1-N1	1.8595(14)	1.8948(10)	1.8343(12)	1.8288(13)	1.8199(9)
Al1-N2	1.8580(13)	1.9108(10)	1.8215(12)	1.8388(13)	1.8336(9)
Al1-N3	1.8926(14)	-	1.7040(13)	1.8561(15)	1.8416(10)
Al1-N4	1.9092(13)	-	-	1.8908(15)	1.8876(8) [v]
N3-N4	1.3731(19)	1.3760(13) [a]	1.352(2) [h]	1.191(2) [m]	1.2002(15)
N4-N5	1.271(2)	1.2688(19) [b]	-	1.192(2) [n]	1.1421(18)
N5-N6	1.387(2)	-	-	1.142(2)	-

Table 1. *Cont.*

	1	**2**	**3**	**4**	**5**
K1-N4	2.7463(14)	2.7647(10) [c]	2.7285(13) [i]	3.0330(16) [o]	-
K1-N5	3.0370(15)	-	-	2.9954(16) [p,q,r]	-
N1-Al1-N2	112.90(6)	101.21(6) [d]	114.69(6)	118.75(6)	116.76(4)
N3-Al1-N6	81.32(6)	81.93(6) [e]	118.31(6) [j]	95.26(7) [s]	96.45(4) [w]
Al1-N3-N4	113.56(11)	112.33(7) [f]	126.90(6) [k]	-	134.96(9)
N3-N4-N5	116.75(14)	116.70(5) [g]	154.44(11) [l]	175.6(2) [t]	175.96(16)
N4-N5-N6	115.08(13)	-	-	176.8(2) [u]	-
N5-N6-Al1	113.24(11)	-	-	-	-

[a] N2-N3; [b] N3-N3[1]; [c] K1-N3; [d] N1-Al1-N1[1]; [e] N2-Al1-N2[1]; [f] Al1-N2-N3; [g] N2-N3-N3[1]; [h] N3-C31;[i] K1-N3; [j] N1-Al1-N3; [k] N2-Al1-N3; [l] Al1-N3-C31; [m] N3-N5; [n] N4-N7; [o] K1-N3[1]; [p] K1-N4[1]; [q] K1-N6 2.9954(16) Å; [r] K1-N8[2] 2.7644(18) Å; [s] N3-Al1-N4; [t] N3-N5-N6; [u] N4-N7-N8; [v] Al1-O1; [w] N3-Al1-O1.
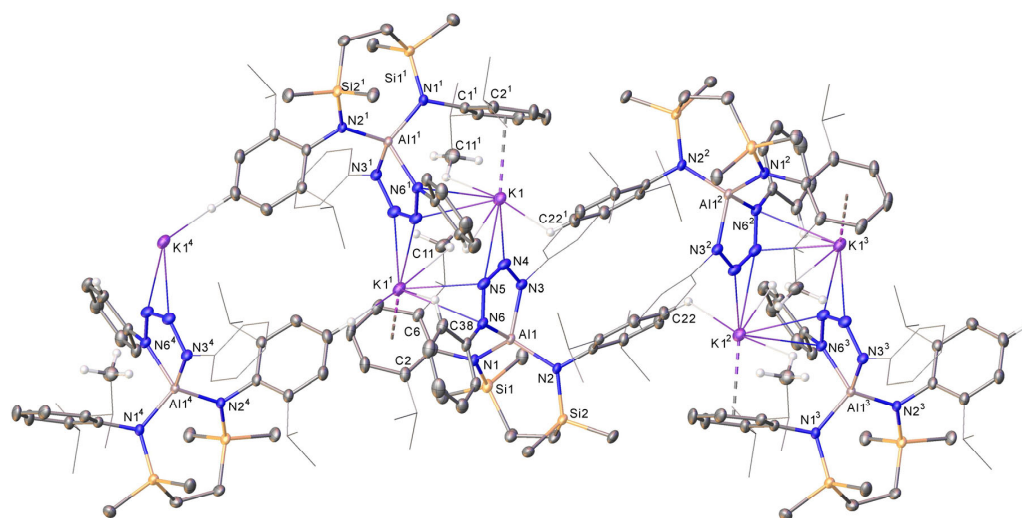

Figure 2. Plot depicting the molecular structure of compound **1**. Ellipsoids are depicted at 30% probability. Minor disordered components and hydrogen atoms (those attached to C11, C22, and C38 excepted) have been omitted and, in addition, peripheral substituents are depicted as wireframes, for perspicuity. Symmetry operations: [1] $1 - x$, y, $3/2 - z$; [2] $1 - x$, $1 - y$, $1 - z$; [3] x, $1 - y$, $-1/2 + z$; [4] x, $1 - y$, $½ + z$.
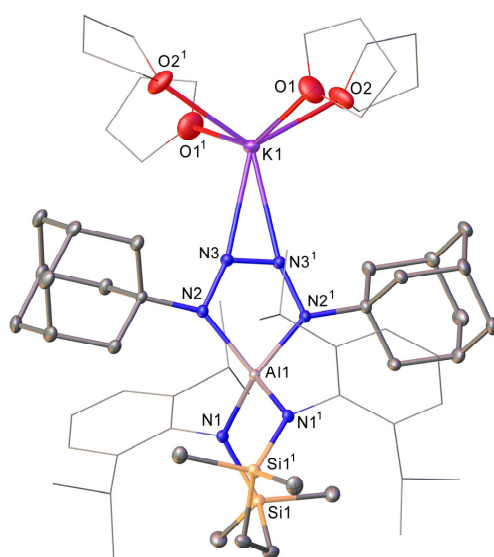

Figure 3. Plot depicting the structure of **2**. Ellipsoids are depicted at 30% probability. Minor disordered components and hydrogen atoms have been omitted and, in addition, peripheral substituents are depicted as wireframes, for clarity. Symmetry operation: [1] $3/2 - x$, y, $1 - z$.

Like the solid-state structure of Aldridge and co-workers' tetrazenylaluminate derivative, $[\{(NON^{xanth})Al(N_4(SiMe_3)_2\}K]_\infty$ [27], compound **1** presents as a 1-dimensionsal polymer (Figure 2), in this case of centrosymmetric molecular dimers. The dimeric units are assembled about two bridging potassium cations (K1 and K1^1), each of which interacts with N4, N5/N4^1, N5^1 (K1-N4 2.7463(14); K1-N5 3.0370(15); K1-N5^1 2.9304(16) Å) of the $\{AlN_4\}$ heterocycle and are further encapsulated by polyhapto engagement with a single *N*-Dipp substituent of each chelated dianion. Polymer propagation parallel to the orthorhombic *c* axis is then achieved via a sequence of intermolecular C-H···potassium contacts between K1/K1^1 and the *para*-situated methine unit of each remaining *N*-Dipp group. Unlike **1**, compound **2** crystallises in the presence of ether solvent and as a molecular contact ion pair (Figure 3). Although the potassium cation (K1) of **2** again interacts strongly with N3 and N3^1 (2.7647(10) Å), further intermolecular interactions are, thus, prevented by *O*-coordination of four molecules of THF. Despite these dissimilarities, the various Al-N and N-N bond lengths and angles about the $\{AlN_4\}$ heterocycles of both compounds **1** and **2** are perturbed only marginally, either in mutual comparison (Table 1) or when appraised against the analogous metric data deduced for $[\{(NON^{xanth})Al(N_4(SiMe_3)_2\}K]_\infty$ [27].

Cognisant of the closely comparable behaviour of both potassium alumanyls **IX** and **XI** toward less sterically demanding azides, we turned our attention to the bulkier mesityl azide that was successfully employed in the synthesis of compound **VI** (Figure 1). Accordingly, treatment of the dimeric potassium alumanyl, **XI**, with two molar equivalents of the azide in benzene again produced a visible gas evolution at room temperature. Subsequent assessment by ^{1}H NMR spectroscopy of the reaction indicated the complete consumption of both reagents and the formation of a single new compound (**3**, Scheme 1), which manifested as a unique, albeit broadened, set of $\{SiN^{Dipp}\}$ ligand and mesityl methyl (δ 2.20 (3H), 1.58 (6H) ppm) environments. Compound **3** could be isolated by slow evaporation of the reaction solvent as single crystals suitable for X-ray diffraction analysis, the results of which are depicted in Figure 4 with selected bond length and angle data presented in Table 1. Like the most closely comparable species, **VI** and **VIIa**, compound **3** comprises a distorted trigonal planar aluminium centre (Σ_{angles} = 359.9°) with N_3Al coordination provided by a combination of the bidentate $\{SiN^{Dipp}\}$ dianion and a terminal arylimido ligand. Unlike both previously reported dimeric potassium arylimidoaluminates, however, compound **3** sequesters a molecule of benzene solvent, which interacts in an η^6-fashion with the potassium cation (K1···benzene$_{cent}$ 2.9740(11) Å) and enforces a monomeric contact ion paired structure. K1 is further encapsulated by a similar interaction with a $\{SiN^{Dipp}\}$ *N*-aryl substituent (K1···benzene$_{cent}$ 2.9064(8) Å) and a close contact to the imido nitrogen atom (K1-N3 2.7285(13) Å). The Al1-N3 bond (1.7040(13) Å) is marginally shorter than the analogous distances reported for either **VI** (1.7251(11) Å) or **VIIa** (1.723(2) Å) and is accompanied by a more obtuse Al1-N3-C31 bond angle (154.44(11) vs. 137.07(9) (**VI**); 146.4(2)° (**VIIa**)). Although these data could be interpreted as indicative of enhanced multiple bond character, in agreement with Aldridge and co-workers' previous calculations [30], we suggest that the contraction of the Al-N$_{imide}$ bond in **3** is more plausibly attributed to a slightly augmented electrostatic interaction resulting from the reduced nuclearity of its structure.

The groups of Aldridge and Goicoechea have also described the use of the $\{NON^{xanth}\}^{2-}$ dianion to achieve the isolation of terminal aluminium imides (**VIIb–VIId**, Figure 1) bearing bulky heteroatom (E = Si, B) substituents at nitrogen [30]. Although superficially analogous to **VI**, **VIIa**, and **3**, the greater lability of the N-E bonds also renders these compounds as viable synthons for the $[N]^{3-}$ anion. With these observations in mind, we speculated that similar Al-N-Al-based nitride structures could be accessible through reaction of **XI** and an appropriately bulky aluminium azide.
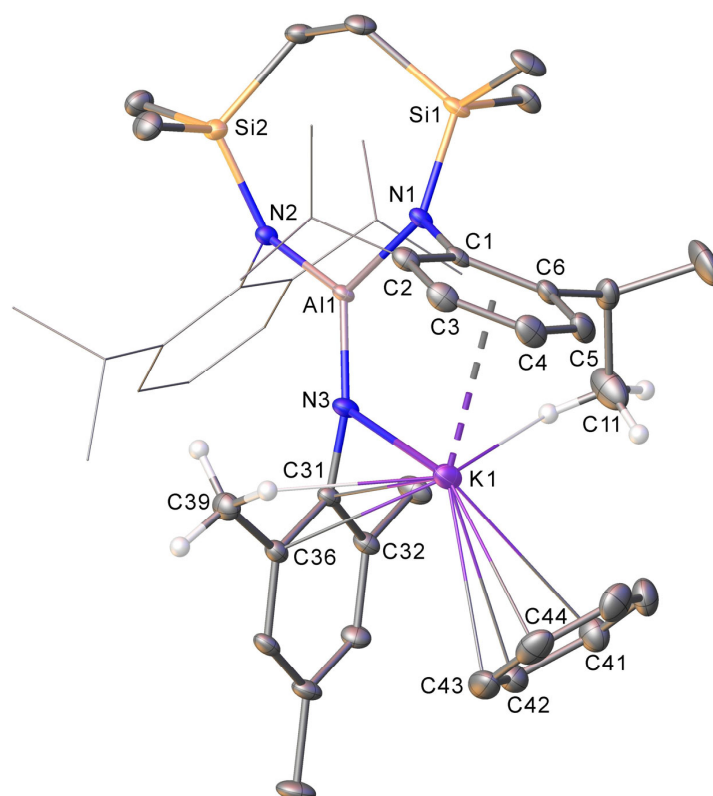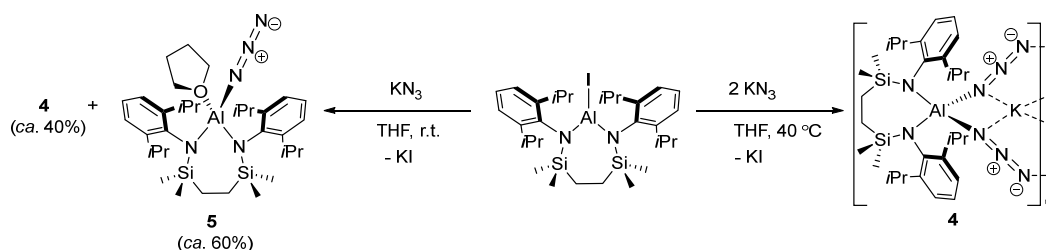
Figure 4. Plot depicting the structure of **3**. Ellipsoids are depicted at 30% probability. In addition to solvent, hydrogen atoms (those attached to C11 and C39 excepted) have been omitted and some peripheral substituents are depicted as wireframes, for visual ease.

An initial reaction of [{SiN^{Dipp}}AlI] and Me$_3$SiN$_3$ in benzene provided no evidence of reaction. The aluminium iodide was, thus, treated with a twofold excess of KN$_3$ in THF at 40 °C for 24 h. This procedure provided a colourless precipitate and a colourless solution, filtration of which yielded compound **4** as a pale yellow powder upon removal of volatiles (Scheme 2). Once isolated, compound **4** was found to be insoluble in either benzene or toluene but redissolved readily in THF. Analysis in d_8-THF by ^{1}H and ^{13}C NMR spectroscopy was consistent with a highly symmetric (C$_{2v}$) structure, an inference that was subsequently supported by X-ray diffraction analysis performed on a single crystal isolated by slow evaporation of a saturated solution of **4** in THF. Compound **4** is a potassium bis(azido)aluminate (Figure 5), which crystallises as a one-dimensional polymer parallel to the *a* axis. This extended structure is propagated via a series of μ-K···N interactions between the alkali metal cations and azide anions, which act as μ-(1,3)-N$_3$ bridging ligands. Although aluminium derivatives coordinated by more than a single azide anion are by no means common, the structure of **4** is otherwise unremarkable and displays bond lengths and angles (Table 1) which are consistent with relevant literature precedents [39–42].

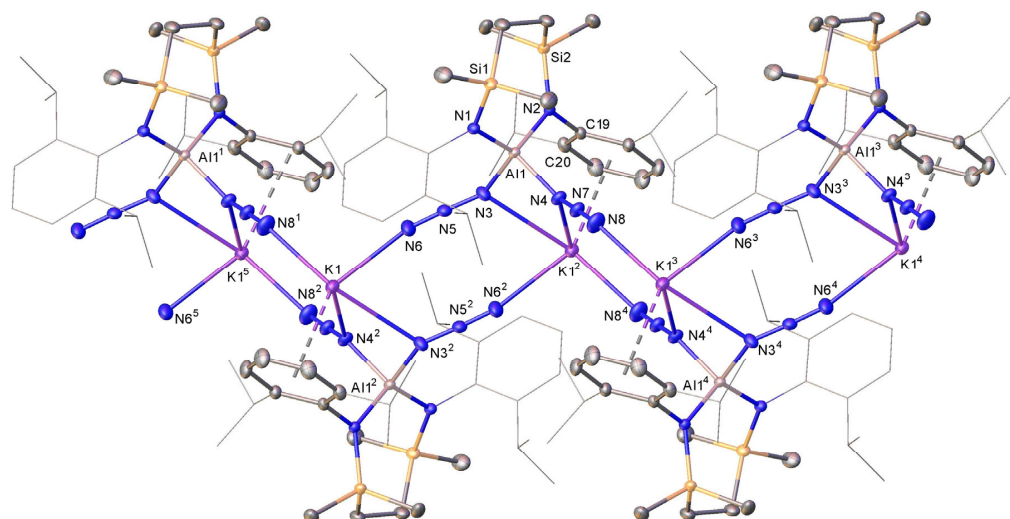**Scheme 2.** Synthesis of compounds **4** and **5**.

Figure 5. Plot depicting the structure of **4**. Ellipsoids are depicted at 30% probability. Hydrogen atoms have been omitted and peripheral substituents are depicted as wireframes, for visual ease. Symmetry operations: ^{1} $-1 + x, y, z$; ^{2} $1 - x, 1 - y, 1 - z$; ^{3} $1 + x, y, z$; ^{4} $2 - x, 1 - y, 1 - z$; ^{5} $-x, 1 - y, 1 - z$.

In a subsequent attempt to achieve the synthesis of a mono(azido)aluminium product, a further reaction was performed on an NMR scale at room temperature in d_8-THF between equimolar quantities of [{SiN$^{\text{Dipp}}$}AlI] and KN$_3$. Assessment of this reaction, which presented as a pale yellow solution and a colourless precipitate, after 2 h by ^{1}H NMR spectroscopy indicated the formation of an approximate 2:3 ratio of **4** and a further new species, compound **5** (Scheme 2), which was readily identifiable in comprising diastereotopic {SiN$^{\text{Dipp}}$} silylmethyl and *N*-Dipp *iso*-propyl substituents, which resonated as two singlets (δ 0.10, 0.09 ppm) and a pair of apparent septets (δ 3.90, 3.78 ppm), respectively. All attempts to fractionally crystallise a bulk sample of **5** for further study of its reactivity were frustrated by its consistent contamination with significant quantities of **4**. A pure sample of **5** sufficient for characterisation was, however, isolated by mechanical separation of the colourless block single crystals obtained by slow diffusion of *n*-hexane into a THF solution. The resultant X-ray diffraction analysis identified **5** as the THF adduct of the desired monoazidoaluminium product (Figure 6), the most salient features of which are congruent with the comparable metric data provided by **4** (Table 1).
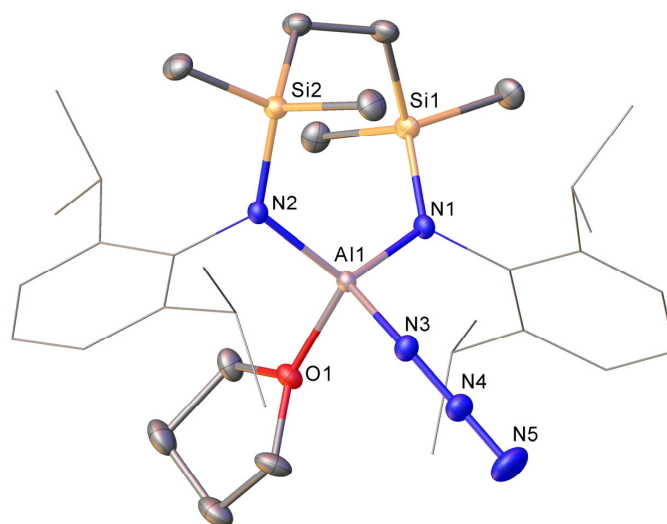

Figure 6. Plot depicting the structure of **5**. Ellipsoids are depicted at 30% probability. Hydrogen atoms have been omitted and peripheral substituents are depicted as wireframes, for clarity.

The unavailability of workable quantities of **5** prompted us to direct our attention back to the potential of the bis-azidoaluminate, compound **4**. Although attempted reactions between compounds **XI** and **4** in both THF or as a suspension in benzene provided visible evidence of gas evolution, analysis by NMR spectroscopy was, in both cases, indicative of the formation of an intractable mixture of products (Figures S21 and S22).

3. Materials and Methods

3.1. General Considerations

Except when stated otherwise, all experiments were conducted using standard Schlenk line and/or glovebox techniques under an inert atmosphere of argon. NMR spectra were recorded with an Agilent ProPulse spectrometer (^{1}H at 500 MHz, ^{13}C at 126 MHz). The spectra are referenced relative to residual protio solvent resonances. Elemental analyses were performed at Elemental Microanalysis Ltd., Okehampton, Devon, UK. Due to the air and moisture sensitivity of compounds **1**, **3**, and **4**, however, no meaningful elemental analysis results could be obtained even after multiple attempts. Solvents were dried by passage through a commercially available solvent purification system and stored under argon in ampoules over 4 Å molecular sieves. Benzene-d_6 and THF-d_8 were purchased from Merck and dried over a potassium mirror before distilling and storage over molecular sieves. [{SiN$^{\text{DiPP}}$}AlK]$_2$ (**XI**) and [{SiN$^{\text{DiPP}}$}AlI] were prepared according to reported procedures [32]. Other chemicals were purchased from Merck and used without further purification.

3.2. Syntheses of New Compounds

Synthesis of [{SiN$^{\text{DiPP}}$}Al-κ^2-*N*,*N*′-({N(Ph)}$_2$N$_2$)]K (**1**)

In a J Youngs NMR tube, C$_6$D$_6$ (ca. 0.5 mL) was added to [{SiN$^{\text{DiPP}}$}AlK]$_2$ (**XI**, 28.0 mg, 0.025 mmol), before addition of PhN$_3$ (11.9 mg, 0.10 mmol) to the bright yellow solution via a micropipette. Gas evolution was observed from the resulting reaction mixture, which transformed into a colourless solution within 10 min at room temperature. *In situ* analysis by NMR spectroscopy indicated quantitative transformation into one single new species **1**. The benzene solution was then put under reduced pressure to remove all volatiles, *n*-hexanes (0.4 mL) were added to the waxy residue, and a tiny amount of solid material was removed by filtration. The filtrate was then kept at −30 °C to provide **1** as colourless crystals suitable for X-ray diffraction analysis. Yield 26 mg, 67%. ^{1}H NMR (500 MHz, 298 K, Benzene-d_6) δ 6.98–6.88 (m, 10H, C$_6$*H*$_5$), 6.80 (t, *J* = 7.5 Hz, 2H, *p*-C$_6$*H*$_3$), 6.74 (d, *J* = 7.5 Hz, 4H, *m*-C$_6$*H*$_3$), 4.25–3.86 (m, 4H, C*H*Me$_2$), 1.30 (d, *J* = 6.7 Hz, 12H, CH*Me*$_2$), 1.27 (s, 4H, SiC*H*$_2$), 0.62 (d, *J* = 6.7 Hz, 12H, CH*Me*$_2$), 0.34 (s, 12H, Si*Me*$_2$). ^{13}C{^{1}H} NMR (126 MHz, 298 K, Benzene-d_6) δ 149.6, 149.2, 147.5 (*i*- and *o*-C$_6$H$_5$), 140.4 (*i*-C$_6$H$_5$), 129.9 (C$_6$H$_5$), 129.3 (C$_6$H$_5$), 124.9 (C$_6$H$_5$), 124.2 (C$_6$H$_5$), 123.3 (*m*-C$_6$H$_3$), 123.0 (*m*-C$_6$H$_3$), 122.6 (C$_6$H$_5$), 119.2 (*p*-C$_6$H$_3$), 27.4 (CHMe$_2$), 26.2 (CH*Me*$_2$), 25.6 (CH*Me*$_2$), 15.3 (SiCH$_2$), 3.4 (Si*Me*$_2$).

Synthesis of [{SiN$^{\text{DiPP}}$}Al-κ^2-*N*,*N*′-({N(Ad)}$_2$N$_2$)][K(THF)$_4$] (**2**)

In a J Youngs NMR tube, C$_6$D$_6$ (ca. 0.5 mL) was added to [{SiN$^{\text{DiPP}}$}AlK]$_2$ (**XI**, 28.0 mg, 0.025 mmol), before the addition of 1-azidoadamantane, (AdN$_3$, 17.8 mg, 0.10 mmol) to the bright yellow solution. Gas evolution was observed from the resulting reaction mixture, which turned pale red with a large amount of colourless amorphous precipitate within 5 min at room temperature. THF (0.2 mL) was then added to the suspension to provide a clear homogeneous solution. The solution was transferred to a vial and was carefully layered with *n*-hexane (0.5 mL). Keeping the vial at room temperature for 3 days provided compound **2** as colourless crystals suitable for X-ray diffraction analysis. The colourless crystals were collected, washed with *n*-hexane (3 × 0.3 mL), and dried *in vacuo* to afford **2** as a colourless powder. Yield: 33.7 mg, 76%. Anal. Cal'd. for C$_{66}$H$_{108}$AlKN$_6$O$_4$Si$_2$ (**2**,

1171.88): C, 67.65%; H, 9.29%; N, 7.17%. Found: C, 67.32%; H, 8.97%, N, 7.28%. ^{1}H NMR (500 MHz, 298 K, d_8-THF) δ 7.03 (dd, *J* = 7.6, 1.9 Hz, 2H, *m*-C$_6$*H*$_3$), 6.85 (dd, *J* = 7.6, 1.9 Hz, 2H, *m*-C$_6$*H*$_3$), 6.76 (t, *J* = 7.6 Hz, 2H, *p*-C$_6$*H*$_3$), 4.21 (sept, *J* = 6.6 Hz, 2H, C*H*Me$_2$), 4.09 (sept, *J* = 6.7 Hz, 2H, C*H*Me$_2$), 1.82–1.75* (m, 12H, C*H*$_2$ on Ad)*overlapping with coordinated residual protio-THF, 1.57 (s br, 3H, C*H* on Ad), 1.55 (s br, 3H, C*H* on Ad), 1.51–1.41 (m, 12H, C*H*$_2$ on Ad), 1.37 (s, 4H, SiC*H*$_2$), 1.35 (d, *J* = 6.4 Hz, 6H, CH*Me*$_2$) 1.23 (d, *J* = 6.5 Hz, 6H, CH*Me*$_2$), 0.97 (d, *J* = 6.7 Hz, 6H, CH*Me*$_2$), 0.92 (d, *J* = 6.6 Hz, 6H, CH*Me*$_2$), 0.54 (s, 6H, Si*Me*$_2$), −0.43 (s, 6H, Si*Me*$_2$). Coordinated residual protio-THF is also observed in the ^{1}H NMR spectrum at 3.62 ppm. ^{13}C{^{1}H} NMR (126 MHz, 298 K, d_8-THF) δ 153.5 (*i*-C$_6$H$_3$), 148.2 (*o*-C$_6$H$_3$), 146.7 (*o*-C$_6$H$_3$), 125.3 (*m*-C$_6$H$_3$), 124.8 (*m*-C$_6$H$_3$), 121.9 (*p*-C$_6$H$_3$), 55.1 (*i*-C on Ad), 44.9 (CH on Ad), 37.9 (CH$_2$ on Ad), 31.3 (CH$_2$ on Ad), 29.1 (CHMe$_2$), 28.3 (CHMe$_2$), 28.2 (CH*Me*$_2$), 26.6 (CH*Me*$_2$), 26.3 (CH *Me*$_2$), 26.0 (CH*Me*$_2$), 16.8 (SiCH$_2$), 9.4 (Si*Me*$_2$), 5.3 (Si*Me*$_2$).

Synthesis of [({SiN^{DiPP}}Al)NMes]K (**3**)

In a J Youngs NMR tube, C$_6$D$_6$ (ca. 0.5 mL) was added to [{SiN^{DiPP}}AlK]$_2$ (**XI**, 28.0 mg, 0.025 mmol), before addition of MesN$_3$ (8.0 mg, 0.050 mmol) to the bright yellow solution via a micropipette. Gas evolution was observed and the reaction mixture transformed into a colourless solution within 10 min at room temperature. The reaction mixture was kept at room temperature for 2 h before all volatiles were removed *in vacuo*. The residue was then dissolved in *n*-hexane (0.6 mL), and slow evaporation of the resultant solution provided colourless crystals suitable for X-ray diffraction analysis. All the crystalline materials were collected and washed with hexane (0.2 mL × 2) and dried under vacuum, providing **3** as a colourless solid. Yield 22 mg, 63%. ^{1}H NMR (500 MHz, 298 K, Benzene-d_6) δ 7.03–6.75 (m, 6H, C$_6$*H*$_3$), 6.66 (s, 2H, C$_6$*H*$_2$Me$_3$), 4.20–3.85 (br, 4H, C*H*Me$_2$), 2.20 (s, 3H, *p*-C$_6$H$_2$*Me*$_3$), 1.58 (s, 6H, *o*-C$_6$H$_2$*Me*$_3$), 1.31 (d, *J* = 6.8 Hz, 12H, CH*Me*$_2$), 1.28–1.22 (m, 6H, CH*Me*$_2$), 1.22–1.03 (m, 10H, CH*Me*$_2$ and SiC*H*$_2$), 0.45–0.00 (br, 12H, Si*Me*$_2$). ^{13}C{^{1}H} NMR (126 MHz, 298 K, Benzene-d_6) δ 157.0 (4° Ar*C* on MesN), 148.8 (4° Ar*C* on C$_6$H$_3$), 147.3 (4° Ar*C* on C$_6$H$_3$), 129.5 (*m*-C$_6$H$_2$Me$_3$), 124.9 (4° Ar*C* on MesN), 124.4 (*m*-C$_6$H$_3$), 123.5 (4° Ar*C* on MesN), 115.6 (*p*-C$_6$H$_3$), 28.2, 26.1, 25.2 (CHMe$_2$ and CH*Me*$_2$), 23.9 (*o*-C$_6$H$_2$*Me*$_3$), 20.9 (*p*-C$_6$H$_2$*Me*$_3$), 14.7 (SiCH$_2$), 1.0 (Si*Me*$_2$). *Hexane impurity observed in the spectra.

Synthesis of [({SiN^{DiPP}}Al)(N$_3$)$_2$]K (**4**)

[{SiN^{DiPP}}AlI] (1.30 g, 2 mmol) and KN$_3$ (320 mg, 4 mmol) were charged into a Schlenk flask. THF (50 mL) was then added to the reaction vessel via a cannula to afford a pale-red solution with a white suspension. The reaction mixture was stirred at 40 °C for 24 h to provide a colourless solution and a white precipitate. The solution was then filtered with a filter cannula, and the filtrate was collected and put under reduced pressure to remove all volatiles. The resultant waxy solid was extracted into THF/toluene (40 mL/20mL), and a minor amount of brown precipitate was removed by filtration. All volatiles were removed *in vacuo* from the filtrate to afford compound **4** as a pale-yellow powder. Yield 1.05 g, 81%. Colourless single needle crystals of **4** suitable for X-ray diffraction analysis were obtained by slow evaporation of a saturated solution in THF. ^{1}H NMR (500 MHz, 298 K, THF-d_8) δ 6.93 (d, *J* = 7.5 Hz, 4H, *m*-C$_6$*H*$_3$), 6.80 (t, *J* = 7.5 Hz, 2H, *p*-C$_6$*H*$_3$), 4.02 (sept, *J* = 6.8 Hz, 4H, C*H*Me$_2$), 1.27 (d, *J* = 6.8 Hz, 12H, CH*Me*$_2$), 1.17 (d, *J* = 6.8 Hz, 12H, CH*Me*$_2$), 0.90 (s, 4H, SiC*H*$_2$), −0.07 (s, 12H, Si*Me*$_2$). ^{13}C{^{1}H} NMR (126 MHz, 298 K, THF-d_8) δ 147.7 (*o*-C$_6$H$_3$), 147.6 (*i*-C$_6$H$_3$), 123.7 (*m*-C$_6$H$_3$), 122.5 (*p*-C$_6$H$_3$), 28.3 (CHMe$_2$), 25.9 (CH*Me*$_2$), 25.8 (CH*Me*$_2$), 15.2 (SiCH$_2$), 1.1 (Si*Me*$_2$).

Isolation of [({SiN^{DiPP}}Al)N$_3$(THF)] (**5**)

In a J Youngs NMR tube, d_8-THF (ca. 0.5 mL) was added to a mixture of [{SiN^{DiPP}}AlI] (32.5 mg, 0.05 mmol) and KN$_3$ (4 mg, 0.05 mmol). The pale-yellow reaction mixture (with white precipitates) was then sonicated at room temperature for 2 h before being analysed by ^{1}H NMR spectroscopy, which indicated the formation of two species, one of which

was identified as **4**. Slow diffusion of *n*-hexane into the THF solution at $-30\ ^\circ$C provided [({SiN$^{\text{Dipp}}$}Al)(N$_3$)$_2$]K (**4**) as a colourless amorphous powder and [({SiN$^{\text{Dipp}}$}Al)N$_3$(THF)] (**5**) as colourless crystalline blocks suitable for X-ray diffraction analysis. An NMR sample of **5** was prepared by mechanical separation of the crystals, which were dissolved in d_8-THF. ^{1}H NMR (500 MHz, 298 K, THF-d_8) δ 7.09 (dd, J = 7.6, 1.8 Hz, 2H, *m*-C$_6$*H*$_3$), 7.04 (dd, J = 7.6, 1.8 Hz, 2H, *m*-C$_6$*H*$_3$), 6.97 (t, J = 7.6 Hz, 2H, *p*-C$_6$*H*$_3$), 3.90 (sept, J = 6.8 Hz, 2H, C*H*Me$_2$), 3.78 (sept, J = 6.8 Hz, 2H, C*H*Me$_2$), 1.33 (d, J = 6.8 Hz, 6H, CH*Me*$_2$), 1.20 (d, J = 6.8 Hz, 12H,CH*Me*$_2$), 1.17 (d, J = 6.8 Hz, 6H, CH*Me*$_2$), 1.06 (s br, 4H, SiC*H*$_2$), 0.10 (s, 6H, Si*Me*$_2$), 0.09 (s, 6H, Si*Me*$_2$). ^{13}C{^{1}H} NMR (126 MHz, 298 K, THF-d_8) δ 148.0 (*i*-C$_6$H$_3$), 146.6 (*o*-C$_6$H$_3$), 146.4 (*o*-C$_6$H$_3$), 125.3 (*p*-C$_6$H$_3$), 124.6 (*m*-C$_6$H$_3$), 124.3 (*m*-C$_6$H$_3$), 32.7 (CHMe$_2$), 30.8 (CHMe$_2$), 28.7 (CH*Me*$_2$), 28.1 (CH*Me*$_2$), 26.7 (CH*Me*$_2$), 26.6 (CH*Me*$_2$), 15.0 (SiCH$_2$), 2.1 (Si*Me*$_2$), 1.7 (Si*Me*$_2$).

4. Conclusions

In summary, the potassium alumanyl, [{SiN$^{\text{Dipp}}$}AlK]$_2$, reacts with organic azides through N$_2$ elimination. In common with earlier reports, whereas less sterically demanding organic azides react with the initially formed imidoaluminate through [2 + 3] cycloaddition to provide the corresponding tetrazenylaluminate products, the terminal imide function may be characterised through recourse to the bulkier *N*-mesityl substituent. In contrast to previously reported derivatives of this type, [{SiN$^{\text{Dipp}}$}AlN(2,4,6-Me$_3$C$_6$H$_2$)(K·C$_6$H$_6$)] crystallises as a molecular monomer through the sequestration of a molecule of benzene solvent and displays a short Al-N bond length of 1.7040(13) Å. Although reactions of [{SiN$^{\text{Dipp}}$}AlI] with KN$_3$ result in metathesis of the iodide and azide anions, the viability of this route to the desired molecular azide is limited by its onward reaction with further KN$_3$, irrespective of the reaction stoichiometry, and the formation of the bis(azido)aluminate derivative [({SiN$^{\text{Dipp}}$}Al)(N$_3$)$_2$]K.

References

1. Azad Malik, M.; O'Brien, P. III–V and Related Semiconductor Materials. In *The Group 13 Metals Aluminium, Gallium, Indium and Thallium: Chemical Patterns and Peculiarities*; Wiley: Hoboken, NJ, USA, 2011; pp. 612–653.
2. Jegier, J.A.; Gladfelter, W.L. The use of aluminum and gallium hydrides in materials science. *Coord. Chem. Rev.* **2000**, *206–207*, 631–650. [CrossRef]

3. Power, P.P. Homonuclear multiple bonding in heavier main group elements. *J. Chem. Soc. Dalton Trans.* **1998**, 2939–2951. [CrossRef]

4. Fischer, R.C.; Power, P.P. Pi-Bonding and the Lone Pair Effect in Multiple Bonds Involving Heavier Main Group Elements: Developments in the New Millennium. *Chem. Rev.* **2010**, *110*, 3877–3923. [CrossRef] [PubMed]

5. Waggoner, K.M.; Hope, H.; Power, P.P. Synthesis and Structure of [MeAlN(2,6-iPr$_2$C$_6$H$_3$)]$_3$: An Aluminum-Nitrogen Analogue of Borazine. *Angew. Chem. Int. Ed. Engl.* **1988**, *27*, 1699–1700. [CrossRef]

6. Wehmschulte, R.J.; Power, P.P. Reactions of (H$_2$AlMes*)2 (Mes* = 2,4,6-(*t*-Bu)$_3$C$_6$H$_2$) with H$_2$EAr (E = N, P, or As; Ar = aryl): Characterization of the Ring Compounds (Mes*AlNPh)$_2$ and (Mes*AlEPh)$_3$ (E = P or As). *J. Am. Chem. Soc.* **1996**, *118*, 791–797. [CrossRef]

7. Laubengayer, A.W.; Smith, J.D.; Ehrlich, G.G. Aluminum-Nitrogen Polymers by Condensation Reactions 1. *J. Am. Chem. Soc.* **1961**, *83*, 542–546. [CrossRef]

8. Amirkhalili, S.; Hitchcock, P.B.; Smith, J.D. Complexes of organoaluminium compounds. Part 10. Crystal and molecular structures of the cage compounds bis-μ-methylamido-hexa-μ$_3$-methylimido-bis(dimethylaluminium)-hexakis(methylaluminium) and bis-μ-methylamido-hexa-μ$_3$-methylimido-bis(dimethylgallium)-hexakis-(methylgallium). *J. Chem. Soc. Dalton Trans.* **1979**, *7*, 1206–1212.

9. Cesari, M.; Perego, G.; Del Piero, G.; Cucinella, S.; Cernia, E. The chemistry and the stereochemistry of poly(N-alkyliminoalanes): II. The crystal and molecular structure of the hexamer, (HAlN-*i*-Pr)$_6$. *J. Organometal. Chem.* **1974**, *78*, 203–213. [CrossRef]

10. Del Piero, G.; Cesari, M.; Dossi, G.; Mazzei, A. The chemistry and the stereochemistry of poly(n-alkyliminoalanes): X. The crystal and molecular structure of the tetramers (HAlN-*i*-Pr)$_4$ and (MeAlN-*i*-Pr)$_4$. *J. Organometal. Chem.* **1977**, *129*, 281–288. [CrossRef]

11. Del Piero, G.; Cesari, M.; Perego, G.; Cucinella, S.; Cernia, E. The chemistry and the stereochemistry of poly (N-alkyliminoalanes): XI. The crystal and molecular structure of the hexamer (HAlN-*n*-Pr)$_6$ and the octamer (HAlN-*n*-Pr)$_8$. *J. Organometal. Chem.* **1977**, *129*, 289–298. [CrossRef]

12. Belgardt, T.; Waezsada, S.D.; Roesky, H.W.; Gornitzka, H.; Haeming, L.; Stalke, D. Synthesis and Characterization of (Pentafluorophenyl)amino-Based Amino- and Iminometallanes. Crystal Structures of (MeAlNC$_6$F$_5$)$_4$ and NHC$_6$F$_5$Ga(MesGa)$_3$(μ$_3$-NC$_6$F$_5$)$_4$ (Mes = 2,4,6-Me$_3$C$_6$H$_2$). *Inorg. Chem.* **1994**, *33*, 6247–6251. [CrossRef]

13. Schulz, S.; Häming, L.; Herbst-Irmer, R.; Roesky, H.W.; Sheldrick, G.M. Synthesis and Structure of the First Dimeric Iminoalane Containing an Al$_2$N$_2$ Heterocycle. *Angew. Chem. Int. Ed. Engl.* **1994**, *33*, 969–970. [CrossRef]

14. Schulz, S.; Voigt, A.; Roesky, H.W.; Häming, L.; Herbst-Irmer, R. Synthesis of Dimeric Iminoalanes by Oxidative Addition of Azides to (Cp*Al)$_4$: Structural Characterization of (Cp*AlNSi*t*Bu$_3$)$_2$ (Cp* = C$_5$Me$_5$). *Organometallics* **1996**, *15*, 5252–5253. [CrossRef]

15. Fisher, J.D.; Shapiro, P.J.; Yap, G.P.A.; Rheingold, A.L. [CpAlN(2,6-*i*-Pr$_2$C$_6$H$_3$)]$_2$: A Dimeric Iminoalane Obtained by Alkane Elimination. *Inorg. Chem.* **1996**, *35*, 271–272. [CrossRef] [PubMed]

16. Hamilton, T.P.; Shaikh, A.W. Theoretical Study of the Dimerization of Multiply-Bonded Aluminum−Nitrogen Compounds. *Inorg. Chem.* **1997**, *36*, 754–755. [CrossRef]

17. Cui, C.; Roesky, H.W.; Schmidt, H.-G.; Noltemeyer, M. [HC{(CMe)(NAr)}$_2$]Al[(NSiMe$_3$)$_2$N$_2$] (Ar = 2,6-iPr$_2$C$_6$H$_3$): The First Five-Membered AlN$_4$ Ring System. *Angew. Chem. Int. Ed.* **2000**, *39*, 4531–4533. [CrossRef]

18. Zhu, H.; Yang, Z.; Magull, J.; Roesky, H.W.; Schmidt, H.-G.; Noltemeyer, M. Syntheses and Structural Characterization of a LAl(N$_3$)N[μ-Si(N$_3$)(*t*Bu)]$_2$NAl(N$_3$)L and a Monomeric Aluminum Hydride Amide LAlH(NHAr) (L = HC[(CMe)(NAr)]$_2$, Ar = 2,6-iPr$_2$C$_6$H$_3$). *Organometallics* **2005**, *24*, 6420–6425. [CrossRef]

19. Hardman, N.J.; Cui, C.M.; Roesky, H.W.; Fink, W.H.; Power, P.P. Stable, monomeric imides of aluminum and gallium: Synthesis and characterization of {HC(MeCDippN)$_2$)}MN-2,6-Trip$_2$C$_6$H$_3$ (M = Al or Ga; Dipp = 2,6-iPr$_2$C$_6$H$_3$; Trip = 2,4,6-iPr$_3$C$_6$H$_2$). *Angew. Chem. Int. Ed.* **2001**, *40*, 2172–2174. [CrossRef]

20. Zhu, H.; Chai, J.; Chandrasekhar, V.; Roesky, H.W.; Magull, J.; Vidovic, D.; Schmidt, H.-G.; Noltemeyer, M.; Power, P.P.; Merrill, W.A. Two Types of Intramolecular Addition of an Al−N Multiple-Bonded Monomer LAlNAr′ Arising from the Reaction of LAl with N$_3$Ar′ (L = HC[(CMe)(NAr)]$_2$, Ar′ = 2,6-Ar$_2$C$_6$H$_3$, Ar = 2,6-iPr$_2$C$_6$H$_3$). *J. Am. Chem. Soc.* **2004**, *126*, 9472–9473. [CrossRef]

21. Li, J.F.; Li, X.F.; Huang, W.; Hu, H.F.; Zhang, J.Y.; Cui, C.M. Synthesis, Structure, and Reactivity of a Monomeric Imino-alane. *Chem. Eur. J.* **2012**, *18*, 15263–15266. [CrossRef]

22. Schwamm, R.J.; Anker, M.D.; Lein, M.; Coles, M.P. Reduction vs. Addition: The Reaction of an Aluminyl Anion with 1,3,5,7-Cyclooctatetraene. *Angew. Chem. Int. Ed. Engl.* **2018**, *58*, 1489–1493. [CrossRef] [PubMed]

23. Anker, M.D.; Schwamm, R.J.; Coles, M.P. Synthesis and reactivity of a terminal aluminium–imide bond. *Chem. Commun.* **2020**, *56*, 2288–2291. [CrossRef] [PubMed]

24. Coles, M.P.; Evans, M.J. The emerging chemistry of the aluminyl anion. *Chem. Commun.* **2022**, *59*, 503–519. [CrossRef]

25. Coles, M.P. Aluminyl Anions. In *Encyclopedia of Inorganic and Bioinorganic Chemistry*; Wiley: Hoboken, NJ, USA, 2024; pp. 1–23.

26. Hicks, J.; Vasko, P.; Goicoechea, J.M.; Aldridge, S. Synthesis, structure and reaction chemistry of a nucleophilic aluminyl anion. *Nature* **2018**, *557*, 92–95. [CrossRef]

27. Heilmann, A.; Hicks, J.; Vasko, P.; Goicoechea, J.M.; Aldridge, S. Carbon Monoxide Activation by a Molecular Aluminium Imide: C−O Bond Cleavage and C−C Bond Formation. *Angew. Chem. Int. Ed. Engl.* **2020**, *59*, 4897–4901. [CrossRef]

28. Hicks, J.; Vasko, P.; Goicoechea, J.M.; Aldridge, S. The Aluminyl Anion: A New Generation of Aluminium Nucleophile. *Angew. Chem. Int. Ed. Engl.* **2020**, *60*, 1702–1713. [CrossRef]

29. Heilmann, A.; Vasko, P.; Hicks, J.; Goicoechea, J.M.; Aldridge, S. An Aluminium Imide as a Transfer Agent for the $[NR]^{2-}$ Function via Metathesis Chemistry. *Chem.–A Eur. J.* **2023**, *29*, e202300018. [CrossRef]

30. Heilmann, A.; Saddington, A.M.; Goicoechea, J.M.; Aldridge, S. Aluminium and Gallium Silylimides as Nitride Sources. *Chem.–A Eur. J.* **2023**, *29*, e202302512. [CrossRef]

31. Queen, J.D.; Irvankoski, S.; Fettinger, J.C.; Tuononen, H.M.; Power, P.P. A Monomeric Aluminum Imide (Iminoalane) with Al–N Triple-Bonding: Bonding Analysis and Dispersion Energy Stabilization. *J. Am. Chem. Soc.* **2021**, *143*, 6351–6356. [CrossRef]

32. Schwamm, R.J.; Coles, M.P.; Hill, M.S.; Mahon, M.F.; McMullin, C.L.; Rajabi, N.A.; Wilson, A.S.S. A Stable Calcium Alumanyl. *Angew. Chem. Int. Ed.* **2020**, *59*, 3928–3932. [CrossRef]

33. Schwamm, R.J.; Hill, M.S.; Liu, H.; Mahon, M.F.; McMullin, C.L.; Rajabi, N.A. Seven-Membered Cyclic Potassium Diamidoalumanyls. *Chem.–A Eur. J.* **2021**, *27*, 14971–14980. [CrossRef] [PubMed]

34. Liu, H.-Y.; Hill, M.S.; Mahon, M.F. Diverse reactivity of an Al(I)-centred anion towards ketones. *Chem. Commun.* **2022**, *58*, 6938–6941. [CrossRef] [PubMed]

35. Liu, H.-Y.; Hill, M.S.; Mahon, M.F.; McMullin, C.L.; Schwamm, R.J. Seven-Membered Cyclic Diamidoalumanyls of Heavier Alkali Metals: Structures and C–H Activation of Arenes. *Organometallics* **2023**, *42*, 2881–2892. [CrossRef] [PubMed]

36. Liu, H.-Y.; Mahon, M.F.; Hill, M.S. Aluminum–Boron Bond Formation by Boron Ester Oxidative Addition at an Alumanyl Anion. *Inorg. Chem.* **2023**, *62*, 15310–15319. [CrossRef]

37. Hill, M.S.; Mahon, M.F.; McMullin, C.L.; Neale, S.E.; Pearce, K.G.; Schwamm, R.J. White Phosphorus Reduction and Oligomerization by a Potassium Diamidoalumanyl. *Z. Anorg. Allg. Chem.* **2022**, *648*, e202200224. [CrossRef]

38. Zhu, L.; Kinjo, R. Reactions of main group compounds with azides forming organic nitrogen-containing species. *Chem. Soc. Rev.* **2023**, *52*, 5563–5606. [CrossRef]

39. Uhl, W.; Gerding, R.; Pohl, S.; Saak, W. Reactions of R_2Al-AlR_2 (R = $CH(SiMe_3)_2$) with trimethylsilyl azide. Insertion into the Al-Al bond and formation of a trimeric dialkylaluminum azide. *Chem. Ber.* **1995**, *128*, 81–85. [CrossRef]

40. Fischer, R.A.; Miehr, A.; Sussek, H.; Pritzkow, H.; Herdtweck, E.; Müller, J.; Ambacher, O.; Metzger, T. Structures of $(C_5H_5N)_3Al(N_3)_3$, $[Me_2N(CH_2)_3]_2Al(N_3)$ and $Me_2(N_3)Al(H_2NBut)$. Low-temperature OMVPE of AlN in the absence of ammonia. *Chem. Commun.* **1996**, *23*, 2685–2686. [CrossRef]

41. Sussek, H.; Stowasser, F.; Pritzkow, H.; Fischer, R.A. Tetraazido Complexes of Aluminium, Gallium, and Indium. *Eur. J. Inorg. Chem.* **2000**, *2000*, 455–461. [CrossRef]

42. Knabel, K.; Nöth, H. Synthesis and Structures of Some Aluminum Pseudohalides. *Z. Naturforschung Sect. B-A J. Chem. Sci.* **2005**, *60*, 155–163. [CrossRef]

43. Dolomanov, O.V.; Bourhis, L.J.; Gildea, R.J.; Howard, J.A.K.; Puschmann, H. OLEX2: A Complete Structure Solution, Refinement and Analysis Program. *J. Appl. Crystallogr.* **2009**, *42*, 339–341. [CrossRef]

44. Sheldrick, G.M. SHELXT-Integrated Space-Group and Crystal-Structure Determination. *Acta Crystallogr. Sect. A Found. Adv.* **2015**, *A71*, 3–8. [CrossRef] [PubMed]

45. Sheldrick, G.M. Crystal Structure Refinement with SHELXL. *Acta Crystallogr. Sect. C Struct. Chem.* **2015**, *C71*, 3–8. [CrossRef]